GAMMA CAMERA COLLIMATOR CONSIDERATIONS FOR IMAGING ^{123}I

Ronald E. McKeighen, Gerd Muehllehner, and Robert A. Moyer

Searle Analytic, Inc., and Searle Radiographics, Inc., Des Plaines, Illinois

Line-spread functions and energy spectra for commercially produced ^{123}I were obtained on an Anger scintillation camera using three different collimators. Images of a thyroid phantom were also obtained using the same collimators. Although the 529-keV gamma ray of ^{123}I has a relative intensity of only about 1%, it and other high-energy but low-abundance gamma rays seriously degrade images by virtue of septum penetration through thin-wall collimators. Use of the pinhole collimator minimizes this problem.

Iodine-123 is regarded as a more ideal radioisotope of iodine than ^{131}I for in vivo measurements, particularly thyroid imaging (*1–5*). Its charged-particle emission is minimal and radiation dose to the patient is much less than with ^{131}I. Iodine-123 has a short half-life (13.3 hr) and the most abundant gamma ray at 159 keV is comparable to the 140-keV gamma of ^{99m}Tc. It might be assumed, therefore, that ^{123}I could be imaged with the same low-energy parallel-hole collimators as used for ^{99m}Tc. However, there are also higher energy gamma-ray transitions from ^{123}I, as well as isotopic impurities such as ^{130}I, ^{124}I, ^{126}I, and ^{131}I (*6–8*). Low-energy collimators are very ineffectual in collimating these higher energy gamma rays, and even though such gamma rays amount to only a small percentage relative to the 159-keV primary gammas at the source, a large fraction of these penetrate the collimator and cause interactions in the scintillation crystal. The problem of septal penetration has previously been discussed by Wellman, et al with respect to scanner collimators and the use of a pinhole collimator on the Anger gamma camera (*2,3*). Photoelectric interactions from high-energy gammas may be eliminated by energy discrimination. At an energy of approximately 500 keV, however, the probability of a Compton-scattering event in the crystal is high. Some of these Compton events will deposit an energy in the crystal that falls within the 159-keV photopeak window of the single-channel analyzer and will therefore not be discriminated against. Image degradation due to this effect was studied using several collimators with the Anger scintillation camera.

MATERIALS AND METHODS

A multichannel analyzer was used in conjunction with an Anger scintillation camera (Searle Radiographics, Inc. Pho/Gamma HP) to obtain data on energy spectra, line-spread function (LSF), and images of a Picker thyroid phantom filled with about ⅓ mCi of ^{123}I. Data were taken on the following Searle Radiographics collimators: (A) high resolution (Part #821741); (B) 4,000-hole collimator (Part #820719); and (C) pinhole collimator (Part #820728). The septa of Collimator A are 0.010-in. thick lead whereas the septa of Collimator B are 0.030-in. thick.

The ^{123}I used for this study was obtained from Medi+Physics, Inc. The radionuclide composition at calibration time was specified as (A) $^{123}I > 95\%$; (B) $^{124}I < 1\%$; (C) $^{126}I < 0.5\%$; (D) $^{130}I < 3\%$; (E) $^{131}I < 0.5\%$. Data were taken within 2–3 hr of calibration time.

The line source consisted of a glass capillary tube 12 in. long having 1.0-mm inside diam, and was filled with approximately ⅓ mCi of ^{123}I. Data for LSF were taken with the line source at a distance of 2 in. from the collimator face. Data were taken both in air and with 1$\frac{3}{16}$-in.-thick Lucite interposed between line source and collimator as scattering material. Data on energy spectra were taken with about ⅓ mCi of ^{123}I in a small glass bottle placed at the

Received Sept.10, 1973; original accepted Nov. 26, 1973.

For reprints contact: R. E. McKeighen, Searle Analytic Inc., Searle Radiographics Inc., 2000 Nuclear Dr., Des Plaines, Ill. 60018.

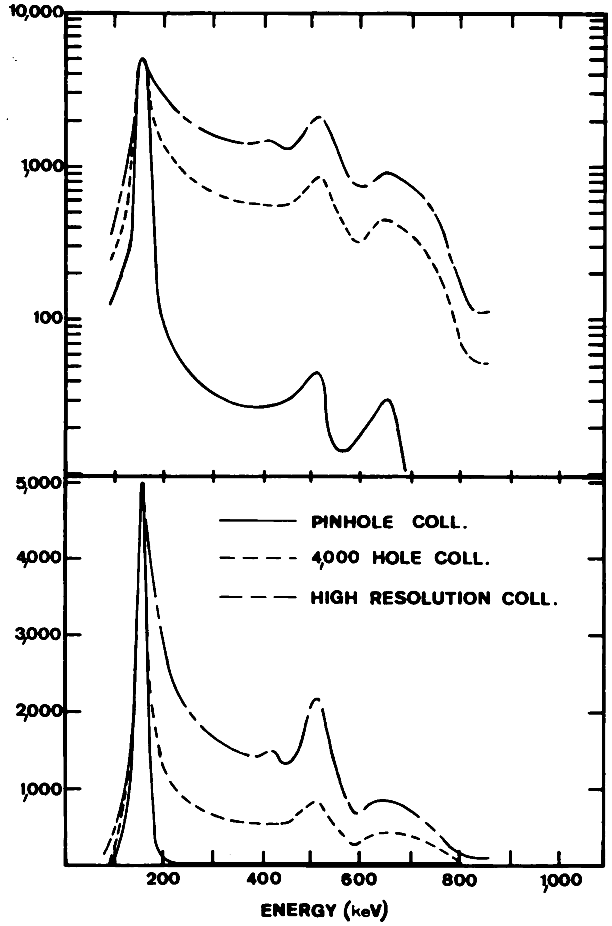

FIG. 1. Energy spectra of Medi+Physics ^{123}I-sodium iodide obtained on Anger scintillation camera through three different collimators in air. Source to collimator distance was 2 in. Top: semi-logarithmic plot; Bottom: linear scale.

same distance. Pictures of a thyroid phantom containing ^{123}I were also taken at the same distance from each collimator.

RESULTS AND DISCUSSION

The energy spectra obtained on the scintillation camera through the various collimators are shown in Fig. 1 in both linear and logarithmic fashion for clarity. For the high-resolution and 4,000-hole collimators the 159-keV photopeak is superimposed upon a high Compton-scattered background from the higher energy gammas, arising both from ^{123}I itself and from other isotopic impurities of iodine. The data of Fig. 1 indicate that the Compton background for the high-resolution collimator is 2½ times that of the 4,000-hole collimator.

For the high-resolution collimator it was empirically determined that only about one-third of the counts falling in the 20% window centered at 159 keV were owing to true 159-keV gamma ray transitions from ^{123}I. The rest came from Compton-scattering events in the scintillation crystal of higher energy gammas, emitted by ^{123}I itself and other impurities, the predominant one being ^{130}I. The gamma-ray transitions from the various isotopes are tabulated in Table 1. The most significant high-energy gamma from ^{123}I is that at 529 keV which occurs in 1.08 out of 100 decays of ^{123}I.

It is well known that scattering in the patient degrades image quality. It should be noted, however, that the degrading effect of the high-energy gammas arises predominantly from Compton scattering in the NaI crystal itself after penetrating the thin-wall septa of the collimator. Since the parallel-hole collimators attenuate the 159-keV gammas by a factor of about 1.2×10^{-4} and 529-keV gammas by only approximately 10^{-1}, the number of 529-keV gammas reaching the NaI crystal compared with the 159-keV gammas will be significant. Whereas the probability of a 159 keV being stopped in a ½-in. NaI crystal is about 80%, the probability of a 510-keV gamma undergoing Compton scattering in the crystal with escape of the secondary photon is also significant, being about 18% (9). Many of these Compton-scattering events will deposit an energy in the crystal that is accepted by the energy analyzer with a window set around the 159-keV photopeak. Although a high-energy gamma could undergo backscattering in the patient and travel toward the camera with an energy close to the 159-keV acceptance window, such gammas would again be greatly attenuated by the collimator.

As well as yielding degraded image quality, use of the high-resolution and 4,000-hole collimators will result in reduced counting-rate capability at high counting rates because of the large number of events outside the acceptance window which have to be evaluated and rejected. From the energy spectra of Fig. 1, it was determined that the ratio of counts falling outside a 20% window centered around the 159-keV photopeak to the number of counts falling inside the window was 6.3 for the high-resolution collimator, 3.3 for the 4,000-hole collimator, and 0.49 for the pinhole collimator. These ratios, however, would be different in the presence of scattering material.

The line-spread function in air for the three different collimators are graphed in Fig. 2. Again, the energy window was 20% centered around the photopeak. For the high-resolution collimator the counts in the wings of the LSF begin at a level corresponding to 15% of the peak counts and are due to the high-energy gammas. In contrast, the septum penetration on the high-resolution collimator for a line source of ^{99m}Tc only begins at the 0.5% level of the counts in the peak. For the 4,000-hole collimator with its 0.30-in. septa, the wings of the LSF

TABLE 1. GAMMA-RAY TRANSITIONS FROM VARIOUS ISOTOPES OF IODINE AND THEIR ABUNDANCE

Isotope	Gamma-ray energy (keV)	No. of transitions/ 100 decays of isotope (or relative intensity in %)*
^{123}I (Ref. 6)	159.0	99.3
	183.7	0.03
	192.7	0.03
	248.3	0.067
	281.0	0.067
	346.6	0.10
	440.4	0.36
	505.6	0.26
	529.0	1.08
	538.5	0.27
	624.9	0.067
	687.7	0.025
	736.1	0.034
	784.4	0.042
^{124}I (Ref. 7)	602.7	100
	645.76	18.0
	722.72	21.0
	890.0	0.4
	968.2	0.8
	1,045.2	0.8
	1,325.6	1.5
	1,368.5	5.0
	1,450.0	1.1
	1,500.0	6.0
	1,691.0	21.0
	1,900.0	0.8
	2,091.1	3.0
	2,293.6	2.3
	2,740.0	0.9
^{126}I (Ref. 8)	388.5	33.0
	492.0	1.9
	666.2	29.1
	753.7	3.7
	880.5	0.7
	1,377.9	0.0012
	1,420.1	0.28
	2,044.1	0.0037
^{130}I (Ref. 7)	419	36
	538	100
	669	100
	743	87
	1,150	12
^{131}I (Ref. 7)	80.16	2.6
	177.19	0.3
	272.45	0.07
	284.31	5.9
	318.14	0.09
	325.80	0.24
	364.49	79.0
	503.13	0.35
	637.01	6.7
	642.80	0.2
	722.92	1.8

* Note that relative intensity in percent is not necessarily the same as No. of transitions/100 decays of the isotope.

amount to about 3% of the peak. The pinhole collimator gives the best LSF with ^{123}I, having wings that begin at a level about 0.5% of the peak counts.

The varying quality of images of a thyroid phantom taken using the different collimators may be seen by examining Fig. 3. The degrading effect of septum penetration is quite apparent in the image taken with the high-resolution collimator; the area surrounding the thyroid contains many counts in the background. Only the largest cold nodule is barely perceptible. The 4,000-hole collimator greatly reduces the background due to septum penetration but the resolution is poor. In contrast, the image of the ^{123}I-filled thyroid phantom taken with the pinhole collimator shows little degradation due to septum penetration and has good resolution. The thick walls of the pinhole collimator greatly reduce the ratio of high-energy gammas to 159-keV gammas getting to the crystal. Scattering material interposed between the ^{123}I source and collimator increased the image degradation but it is again stressed that the predominant effect due to the high-energy gammas is from Compton scattering in the NaI crystal itself and not Compton scattering in the patient or source.

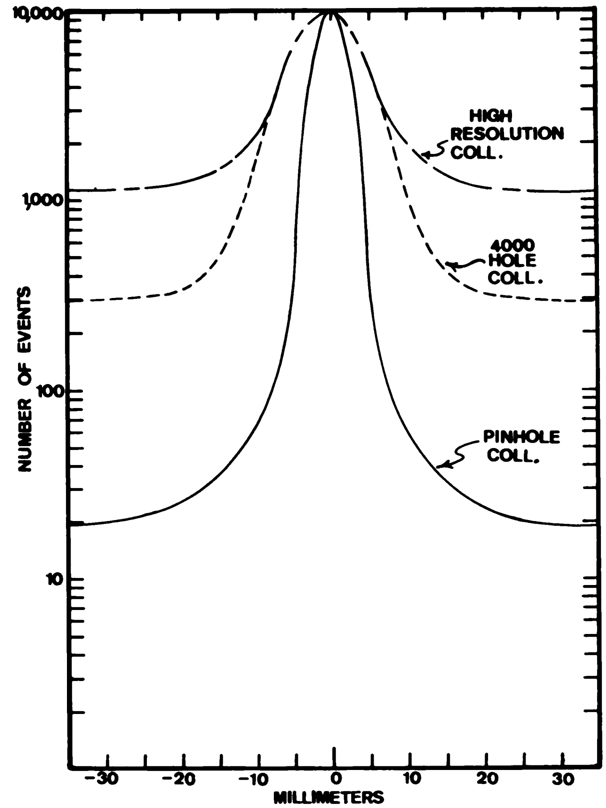

FIG. 2. Line-spread functions (LSF) of ^{123}I-line source on various collimators; line source was 2 in. from collimator in air.

The absorbed patient radiation dose (*10*) associated with the administration of 1 mCi of various isotopes of iodine is given in Table 2. Using maximum allowable radiocontaminant levels at calibration time, the radiation dose to the patient for a 100-μCi aliquot was calculated by Medi+Physics

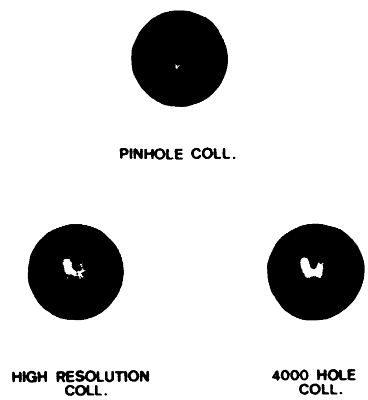

FIG. 3. Images of Picker thyroid phantom obtained with three different collimators at distance of 2 in. in air. Each image contains 100,000 counts.

TABLE 2. ABSORBED RADIATION DOSE ASSOCIATED WITH 1 mCi OF EACH ISOTOPE (*10*)

	Rads/mCi	
Radionuclide	Thyroid	Whole body
^{123}I	20	0.07
^{124}I	1,200	14.2
^{126}I	2,300	5.5
^{130}I	186	0.85
^{131}I	2,100	3.6

for its ^{123}I to be 6 rads to the thyroid and 0.03 rads to the whole body. Although ^{130}I is the highest impurity at approximately 3%, it contributes only about 0.56 rads of the 6-rad dose to the thyroid. It would seem that ^{130}I is not a bothersome impurity from the standpoint of patient dose but rather from the standpoint of collimation. Its half-life of 12.3 hr is almost identical to that of ^{123}I, and it has gamma rays of 419, 538, 669, 743, and 1,150 keV.

Examination of the energy spectrum of the ^{123}I sample measured with a Ge(Li) detector by Medi+Physics indicated that the Compton-scattered background falling in the 159-keV photopeak from gammas attributable to ^{130}I would be about 1.8 times that attributable to higher energy gammas of ^{123}I itself. Contributions from other isotopes were about a factor of 10 lower. It was experimentally determined on the Anger camera that only one-third of the counts in the window were from true 159-keV gamma rays for the source a few inches from the high-resolution collimator. Therefore, it may be roughly estimated that if ^{123}I were to be obtained pure, the fraction of true primary gammas falling in the 159-keV window would only be increased from 35 to 58% in the case of the high-resolution collimator.

In conclusion, satisfactory images of ^{123}I may be obtained for small organs such as the thyroid gland using the pinhole collimator. However, imaging ^{123}I over a large field of view with a thin-wall parallel-hole collimator may result in poor image quality because of septum penetration. The 4,000-hole collimator should give acceptable images in some situations using ^{123}I. It should also be noted that the intrinsic camera resolution for the 159-keV ^{123}I gamma ray is better than for the 140-keV ^{99m}Tc gamma ray. Furthermore, the organ specificity for iodine should also give better clinical image quality using ^{123}I over ^{99m}Tc in thyroid imaging with the pinhole collimator (*1*).

REFERENCES

1. Atkins HL, Klopper JF, Lambrecht RM, et al: A comparison of technetium 99m and iodine 123 for thyroid imaging. *Am J Roentgenol Radium Ther Nucl Med* 117: 195–201, 1973

2. Wellman HN, Mack JF, Saenger EL, et al: A study of the parameters influencing the clinical use of iodine-123. In *Angiography Scintigraphy Symp. European Assoc. Radiology*, Diethelm L, ed, New York, Springer Verlag, 1972, pp 129–137

3. Wellman HN, Anger RT: Radioiodine dosimetry and the use of radioiodines other than ^{131}I in thyroid diagnosis. *Semin Nucl Med* 1: 356–378, 1971

4. Sodd VJ, Wellman HN, Branson BM: ^{123}I thyroid measurements with a Ge(Li) detector. *J Nucl Med* 10: 136–139, 1969

5. Sodd VJ, Scholz KL, Blue JW, et al: Evaluation of nuclear reactions that produce ^{123}I in the cyclotron. *Isot Radiat Technol* 9: 154–159, 1971–72

6. Nuclear Data Sheets, 7: No 4, 370, 1972

7. Heath RL: Table of isotopes. In *Handbook of Chemistry and Physics*, 53rd ed, Cleveland, Chemical Rubber Co, 1972, B-343

8. Nuclear Data Sheets, 9: No 2, 130, 1973

9. Anger HO, Davis DH: Gamma ray detection efficiency and image resolution in sodium iodide. *Rev Sci Instrum* 35: 693–697, 1964

10. Ellis RE: *International Comm Radiol Protec*, Publication 17, New York, Pergamon Press, 1971